IEEE Photonics Journal
An IEEE Photonics Society Publication

BER Analysis of a Deep Space Optical Communication System Based on SNSPD Over Double Generalized Gamma Channel

Volume 10, Number 5, September 2018

Bo Li
Yutong Liu
Shoufeng Tong
Lei Zhang
Haifeng Yao

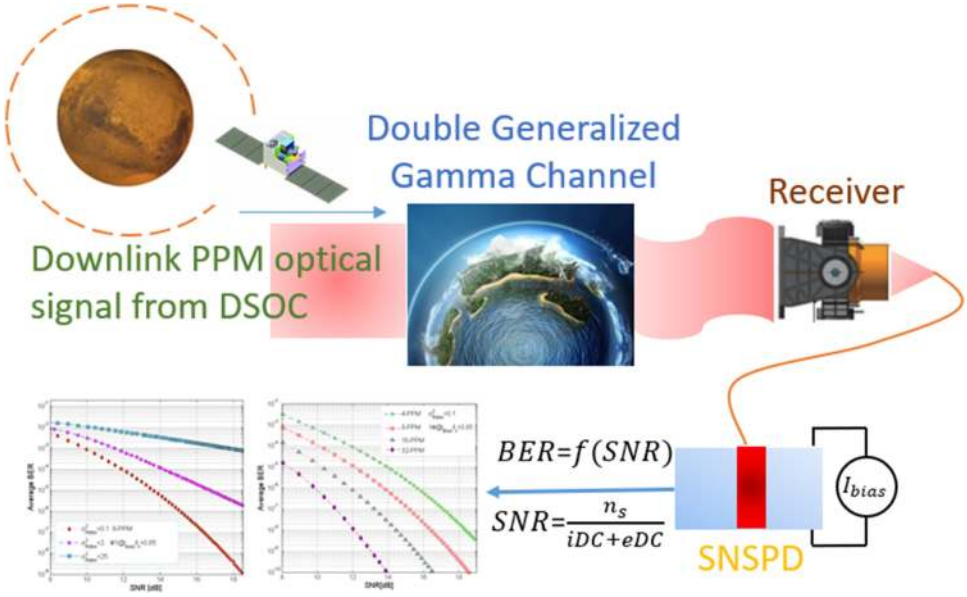

DOI: 10.1109/JPHOT.2018.2868738
1943-0655 © 2018 IEEE

BER Analysis of a Deep Space Optical Communication System Based on SNSPD Over Double Generalized Gamma Channel

Bo Li,[1] **Yutong Liu**,[2] **Shoufeng Tong**,[3] **Lei Zhang**,[3] **and Haifeng Yao**[1]

[1]Institute of Photoelectric Engineering, Changchun University of Science and Technology, Changchun 130022, China
[2]College of optical and Electronical Information, Changchun 130114, China
[3]Institute of Space Photoelectric Technology, Changchun University of Science and Technology, Changchun 130022, China

DOI:10.1109/JPHOT.2018.2868738

Manuscript received August 5, 2018; revised August 29, 2018; accepted August 31, 2018. Date of publication September 13, 2018; date of current version October 10, 2018. Corresponding author: Shoufeng Tong (e-mail: dsphd2017@126.com).

Abstract: Optical communication has a broad prospect in deep space communication. The mechanism and the asymptotic dark count estimate of superconducting nanowire single photon detector (SNSPD) are introduced. Considering the detector bias current, an average bit error expression is established based on SNSPD and pulse position modulation optical communication system over Double Generalized Gamma channel firstly. Numerical results show that both the bias current and the atmospheric turbulence intensity have influence on the BER performance. The uncoded BER can achieve 10–5 in 32-PPM scheme with Ibias/Iv = 0.85 when SNR = 8 dB under weak atmospheric turbulence. This work can be utilized in deep space optical communication and benefits downlink communication system design.

Index Terms: Deep space optical communication, bit error rate (BER), pulse position modulation (PPM), superconducting nanowire single photon detector (SNSPD).

1. Introduction

Compared to microwave communications, the laser communication technique offers an efficient method to meet the ever-increasing demand for data transmission rate in deep space exploration systems [1]. In 2013, NASA's Lunar Laser Communication Demonstration (LLCD) has successfully demonstrated between the Lunar Atmosphere and Dust Environment Explorer (LADEE) and ground stations [2]–[6], the demonstration has achieved almost an order of magnitude higher data rate than the best Ka-band radio. It shows a broad prospect for data rate improvement in deep space. Additionally, the Deep-space Optical Terminals (DOT) for Mars-Earth optical communication [7], [8] and the optical communication project for Sun-Earth Lagrange Point 2 are under research or development [9].

The optical signal from deep space terminals, which suffers the limited transmitting power and huge link loss, only contains several photons when incident on receiving surface. This poses big challenges to the modulation method and detection techniques. In [10]–[13], Pulse position modulation (PPM) has been chosen to provide an energy-efficient means of using high peak power laser for transmitting signals from deep space to earth-based receiving stations. In the 2^M-ary PPM

modulation scheme, each channel symbol period is divided into 2^M equal non-overlapping time slots, and the information comprised of M bits is sent by pulsing the optical intensity in one of these slots. Each slot is very short (∼ns), but the laser power that the signal slot contained is very high (∼kW). Therefore, the PPM can compensate the huge link loss and suppress the background photons, and now it is the preferred technique for DSOC system. PPM can overcome the power restriction on payload and greatly reduce background photons in signal slots.

With the development of single photon detection technology, a variety of high-sensitivity single photon detectors (SPDs) have been developed. Currently, there are two kinds of SPDs have been well applied in DSOC, namely, Geiger Mode-Avalanche Photodiode (GM-APD) and Superconducting Nanowire Single Photon Detector (SNSPD). Owing to its small size and low power consumption, GM-APD is more suitable for satellite platform. But the detector's performances of detection efficiency@1550 nm, dark count rate (DCR) and the dead time are limited. However, SNSPDs have a higher photon detection efficiency (50%∼93%), lower DCR (∼100Hz), low timing jitter (∼ps) and fast reset time (∼ns). Therefore, SNSPDs are the best present technology choice for photon detection in DSOC to improve receiver sensitivity [14]–[20]. Besides, SNSPDs are also widely used in many applications, such as fundamental tests of quantum mechanics, long range 3D infrared depth imaging, integrated circuit testing, quantum key distribution, fibre optic temperature sensing, and singlet oxygen luminescence detection [21]. But due to its large volume and mass, high power consumption, SNSPDs are only applied to the ground station right now. However, next generation miniaturized closed-cycle cooling platforms which are compatible with space applications are under development [21], [22].

It is generally known that the bit rate error (BER) of DSOC has direct relevance to modulation mode, atmospheric condition and detector performance. In [23], the capacity computation and the corresponding BER based on avalanche photodiode detector (APD) and PPM were comprehensively analyzed under different channels. In [24], a simple DSOC BER model based on SNSPD was proposed but without considering the turbulence and modulation. SNSPD is one of key subsystems of ground terminal for deep space optical communication, and a comprehensive BER analysis based on the detector is necessary. Therefore, we firstly carried out an accurate BER calculation formula which takes PPM and Double Generalized Gamma distribution into consideration. As far as we know, there is no similar research on this. We think this work would give some useful and meaningful references for DSOC system. The rest of paper is organized as follows: In Section 2, the origin of dark count of SNSPDs and the Double Generalized Gamma (DGG) distribution are discussed. The symbol error based on SNSPD, PPM and DGG is given, then we drive the corresponding BER formula. Section 3 is devoted to numerical simulation and discussion. Finally conclusions are drawn in Section 4.

2. BER Analysis

When an incident photon interacts with the nanowire which held below its transition temperature and applied a bias current, a hot-spot which comprised of a cloud of excessive quasi-particle (QP) will be induced. It drives a belt-like region across the stripe to the normal state. Then the current between the superconducting stripe edges will be redistributed and it leads to a voltage pulse. After the normal belt cools down, the strip returns into the metastable superconducting state for next detection [25], [26].

Dark counts rate (DCR) is a significant noise source of SNSPD caused by black body radiation of the fiber itself and stray light penetrated into the fiber, which named extrinsic reasons. For reducing the extrinsic dark count rate (eDCR), a cold bulk optical filter was used in [27], but with a low system detection efficiency. In [28], a multi-layer film band-pass filter was integrated onto the SNSPD to suppress the dark counts and the detector exhibited a system detection efficiency of 56% with 1 Hz DCR. Beyond the extrinsic reasons above which have been settled as much as possible, intrinsic dark counts also impact the performance of SNSPD [29]. To date, the origin of intrinsic dark counts have been studied a lot and many possible mechanisms have been proposed [30]–[32]. Recent research shows that both quasiparticle diffusion and vortices play a role in the detection event [33].

However, there is no conclusion on the physics origin of DCR yet. But in [32], the authors gave out a formula to fit the experimental data of iDCR, the data agreed well with theoretical results, and the equation can be expressed as

$$R_{iDC} = \frac{4Tc^2R_WL}{\Phi_0^2\omega}\left(\frac{\pi v^3}{2}\right)^{1/2}\left(\frac{\pi\xi}{\omega}\right)^{v+1}\left[1+\left(\frac{\Phi_0 I_{bias}}{\pi vcT}\right)^2\right]^{\frac{v+1}{2}}\exp\left[\frac{\Phi_0 I_{bias}}{\pi cT}\tan^{-1}\left(\frac{\pi vcT}{\Phi_0 I_{bias}}\right)\right]. \quad (1)$$

where ω and L stand for the width and length of nanowire, T presents the operative temperature, I_{bias} is the applied bias current, Φ_0 is the flux quantum, $R_\square$ is the film's sheet resistance slightly above critical temperature T_c, ν is the parameter depends on bias current, temperature and the characteristic energy of a vortex in thin films, ξ is the coherence length.

Up to now, PPM schemes are preferred in DSOC system to compensate the huge link loss and improve the SNR. Thus the symbol error $P_{s\text{-}DC}$ of SNSPD caused by dark counts and M-ary PPM scheme can be expressed as

$$P_{s-DC} = \frac{M}{4}\frac{(R_{iDC}+R_{eDC})}{R_c}\times \mathrm{erfc}\left(\frac{n_s^2\sqrt{M\log_2 M}}{4n_b}\right). \quad (2)$$

where R_c is the total counts per second, n_s and n_b denote the average number of signal photons and background photons per slot. Regardless of the atmosphere channel, the bit error probability P_b expression of hard-decision decoded M-PPM DSOC system based on SNSPD can be expressed as [34]

$$P_{b-DC} \approx \frac{M}{2(M-1)}P_{s-DC}. \quad (3)$$

Then the numerically stable relationship for BER of M-ary detection in turbulent atmosphere can be established as

$$\begin{aligned} P_{b-Channel}(n_s) &= \int_0^\infty P_{b-DC}f(n_s)dn_s \\ &= \int_0^\infty \frac{M^2}{8(M-1)}\frac{(R_{iDC}+R_{eDC})}{R_c}\times \mathrm{erfc}\left(\frac{n_s^2\sqrt{M\log_2 M}}{4n_b}\right)f(n_s)dn_s. \end{aligned} \quad (4)$$

where $f(n_s)$ presents the PDF of turbulent atmosphere distribution.

Scintillation, which induced by atmospheric turbulence, can severely degrade the DSOC system performance, and several statistical models have been proposed in an effort to model this random phenomenon. In [35], a probability distribution function named Double Generalized Gamma (Double GG), which can more accurately describe the irradiance fluctuations under a wide range of turbulence conditions, was derived. The model demonstrated an excellent match to the simulation data and was clearly superior over the Gamma-Gamma distribution. The PDF expression form of GDD given by the literature can be changed into

$$\begin{aligned} f(n_s) = {} & \frac{\gamma_2 p p^{m_2-1/2}q^{m_1-1/2}(2\pi)^{1-(p+q)/2}n_s^{-1}}{\Gamma(m_1)\Gamma(m_2)} \\ & \times G_{p+q,0}^{0,p+q}\left[\left(\frac{\Omega_2}{n_s^{\gamma_2}}\right)^p\frac{p^p q^q\Omega_1^q}{m_1^q m_2^p}\,\middle|\,\begin{matrix}\Delta(q:1-m_1),\Delta(p:1-m_2)\\ -\end{matrix}\right]. \end{aligned} \quad (5)$$

where $\gamma_i > 0$, $m_i \geq 0.5$ and Ω_i $(i = 1, 2)$ are the GG parameters, $G_{p+q,0}^{0,p+q}[\cdot]$ is the Meijer G-function, p and q are positive integer numbers that satisfy $p/q = \gamma_1/\gamma_2$ and $\Delta(j;x) \triangleq x/j, \ldots, (x+j-1)/j$, $\Gamma(\cdot)$

TABLE 1
Parameters of Nanowires[a]

Sample	ω/nm	L/μm	d/μm	$R_{□}/Ω$	v/μm^{-1}	ξ/nm	T/K	I_c/μA
#1	53.4	73.9	6	445	105.224	3.9	5.5	20.1
#2	82.9	145.1	6	393	117.822	4.33	5.5	31.5

[a]From Physical Review B, 83 4400-4408 (2011).

TABLE 2
Data of Nanowires at Different Bias Currents

Sample	ln(DCR/L)		
	I_{bias}/I_v=0.85	I_{bias}/I_v=0.90	I_{bias}/I_v=0.95
#1	-4.3	0.5	4.9
#2	-8.8	-2.7	2.8

is Gamma function. Subsequently, the BER of the DSOC system can be written as

$$P_{b-Channel}(n_s) = \frac{M}{4}\int_0^{\infty}\frac{1}{\sqrt{\pi}}G_{1,2}^{2,0}\left[\frac{n_s^4 M\log_2 M}{16n_b^2}\middle|\begin{matrix}1\\0,\frac{1}{2}\end{matrix}\right]\times\frac{\gamma_2 p p^{m_2-1/2}q^{m_1-1/2}(2\pi)^{1-(p+q)/2}n_s^{-1}}{\Gamma(m_1)\Gamma(m_2)}$$
$$\times G_{p+q,0}^{0,p+q}\left[\left(\frac{\Omega_2}{n_s^{\gamma_2}}\right)^p\frac{p^p q^q\Omega_1^q}{m_1^q m_2^p}\middle|\begin{matrix}\Delta(q:1-m_1),\Delta(p:1-m_2)\\-\end{matrix}\right]dn_s. \quad (6)$$

According to the calculation properties of Meijer-G function, the formula (6) can be simplified as

$$P_{b-Channel}(n_s) = \frac{M\gamma_2 p p^{m_2-1/2}q^{m_2-1/2}(2\pi)^{1-(p+q)/2}}{8\sqrt{\pi}\Gamma(m_1)\Gamma(m_2)}$$
$$\times H_{p+q+2,1}^{0,p+q+2}\left[\frac{(p\Omega_2)^p(q\Omega_1)^q}{m_1^q m_2^p}\times\left(\frac{M\log_2 M}{16}\right)^{0.5\gamma_2 p}\times SNR^{\gamma_{2p}}\middle|\begin{matrix}(a_1,1),\ldots,(a_{p+q},1),(1,0.5\gamma_2 p),(0.5,0.5\gamma_2 p)\\(0,0.5\gamma_2 p)\end{matrix}\right]. \quad (7)$$

where $H_{2,p+q+1}^{p+q,2}[\cdot]$ is the Fox H-function, $a_n = [\Delta(q{:}1-m1), \Delta(p{:}1-m2)]$, $SNR = n_s/(eDC + iDC)$.

It is obvious that both the operation and material parameters of SNSPD and the atmospheric turbulence conditions have significant influences on communication performance. Therefore, numerical simulations should be conducted to choose optimal parameter values.

3. Numerical Result

In this section, the BER performances of DSOC system which based on SNSPD were obtained in different atmospheric turbulence conditions. Error correction coding is not considered here. For more accurate and convenient simulation, we choose the dimensions and operation parameters of nanowires in literature [32], which detailed in Table 1. Then we can get the data ln(DCR/L) and the DCR of each nanowires at different bias currents, detailed in Table 2 and Fig. 1, respectively.

As it is shown in Fig. 1, regardless the eDCR, the iDCR performance of sample #1 and sample #2 differ widely, and it increases sharply with the increment of bias current I_{bias}. We take sample #2 which has a much better performance than sample #1, as an example. The iDCR at the current ratio 0.85 is about 440 times smaller than that at the 0.9 point. This phenomenon will lead to a bad BER performance in optical communication system.

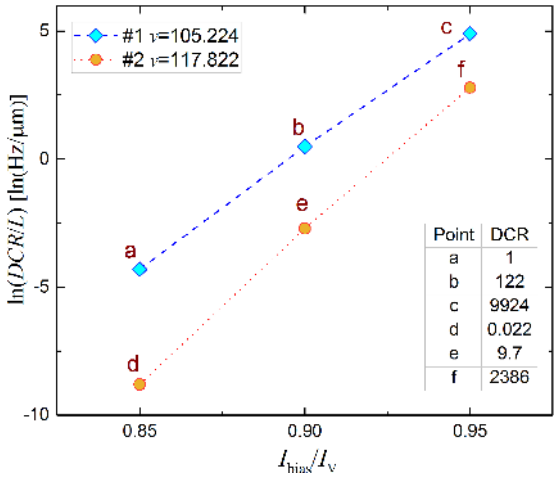

Fig. 1. The DCR of nanowires.

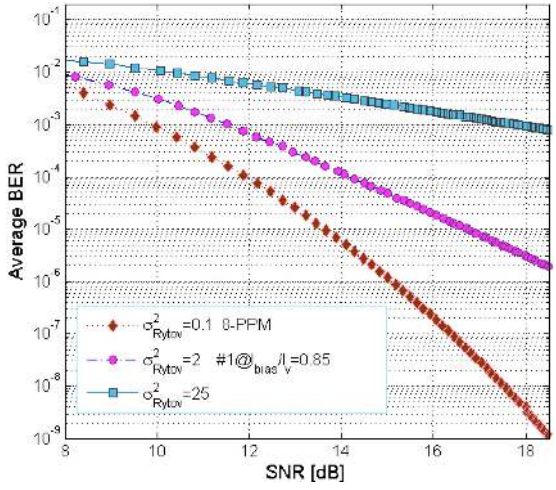

Fig. 2. Average BER under different atmospheric turbulence.

However, in practical applications, the eDCR is much larger than the iDCR even filters are adopted, so we assume that eDCR is 10 times more than iDCR. Fig. 2 shows the average BER as a function of SNR under three different atmospheric turbulence. We assume that the detection efficiency of the sample #1 SNSPD is 60% and the modulation order of the PPM is 8, the parameters of the DGG are listed in Table 3. We can see that strong atmospheric turbulence affects the BER so seriously that there is only a little gain on the communication performance by increasing the SNR. In the 8-PPM scheme, the BER under weak turbulence can achieve 10^{-6} with a 15 dB SNR, but the others are 19 dB and about 40 dB, respectively. It should be noted that, even the 15 dB SNR is difficult to achieve because only few photons could incident on the detector in a DSOC system, so a background noise subtraction method is needed. In [36], an efficient background subtraction algorithms was proposed for DSOC.

Fig. 3 shows the average BER as a function of SNR under weak turbulence and different modulation orders. The system can achieve 10^{-5} BER under the 8 dB SNR in 32-PPM scheme which has a 4 dB gain than the 8-PPM. Clearly, increasing the modulation order is a direct way for performance improvement. But it need to be mindful that, for the same clock frequency and slot time, higher order results in a larger decrease in communication rate. So the choice of M order must be under comprehensive consideration.

TABLE 3
Parameters of Double Generalized Gamma Distribution[b]

Parameter	Weak turbulence	Moderate turbulence	Strong turbulence
σ^2_{Rytov}	0.1	2	25
γ_1	2.1	2.1690	1.8621
γ_2	2.1	0.8530	0.7638
m_1	4	0.55	0.5
m_2	4.5	2.35	1.8
Ω_1	1.0676	1.5793	1.5074
Ω_2	1.06	0.9671	0.9280
p	1	28	17
q	1	11	7

[b]From Journal of Lightwave Technology, 33 2303-2312 (2015).

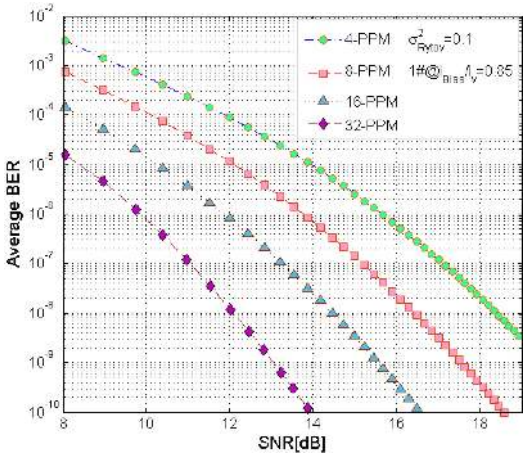

Fig. 3. Average BER in different M-PPM schemes.

4. Conclusion

In this paper, based on the origin of SNSPD dark count rate and the Double Generalized Gamma channel, a theoretical formulation for BER analysis of DSOC system have been developed. With the help of the formulation obtained, we have explored the effects of atmospheric turbulence intensity, PPM order and nanowires parameters on BER performance. Most of the BER is less than the FEC limit of 3.8×10^{-3}, it means that the BER formula can be applied to DSOC. The uncoded BER can achieve 10^{-5} in 32-PPM scheme with $I_{bias}/I_v = 0.85$ when SNR = 8 dB under weak atmospheric turbulence, it has been revealed that a lower bias current can achieve a lower BER, also the communication quality can be improved by choosing a high modulation order and weak atmospheric turbulence condition. Then we can get a more accurate link budget of photon numbers.

References

[1] D. M. Boroson, "Overview and status of the lunar laser communication demonstration," in *Proc. Int. Conf. Space Opt. Syst. Appl.*, 2012, pp. 1–3.
[2] D. M. Boroson, B. S. Robinson, D. V. Murphy, D. A. Burianek, and F. Khatri, "Overview and results of the lunar laser communication demonstration," *Proc. SPIE*, vol. 8971, no. 6, pp. 89710S–11, 2014.

[3] D. M. Boroson and B. S. Robinson, "Status of the lunar laser communication demonstration," *Proc. SPIE*, vol. 8610, no. 861002-1, pp. 1–7, 2013.
[4] B. S. Robinson *et al.*, "The NASA lunar laser communication demonstration –successful high-rate laser communications to and from the Moon," in *Proc. Int. Conf. Space Operations*, 2014, pp. 861002-1–861002-3.
[5] A. Biswas *et al.*, "LLCD operations using the lunar Lasercom OCTL terminal," *Proc. SPIE*, vol. 8971, pp. 450–453, 2014.
[6] W. T. Roberts and M. W. Wright, "The lunar laser OCTL terminal (LLOT) optical systems," *Proc. SPIE*, vol. 8610, no. 8610, pp. 1–9, 2014.
[7] H. Hemmati *et al.*, "Deep-space optical terminals (DOT)," *Proc.SPIE*, vol. 79230, pp. 93–96, 2014.
[8] A. Biswas, H. Hemmati, S. Piazzolla, B. Moision, K. Birnbaum, and K. Quirk, "Deep-space optical terminals (DOT) systems engineering," *Interplanetary Netw. Prog. Rep.*, pp. 42–183, 2010.
[9] K.-J. Schulz and J. Rush, "Optical Link Study Group (OLSG) Final Report," Interagency Operations Advisory Group. Optical Link Study Group, Eur. Space Agency, Paris, France, Tech. Rep. IOAG.T.OLSG.2012.V1A, 2012.
[10] G. kirchner, F. Koidl, D. Kucharski, and W. Steinegger, "Using pulse position modulation in SLR stations to transmit data to satellites," in *Proc. Int. Conf. Telecommun.*, 2011, pp. 447–450.
[11] B. Moision and J. Hamkins, "Deep-space optical communications downlink budget: Modulation and coding," *Interplanetary Netw. Prog. Rep.*, vol. 154, no. 50, pp. 17674–17680, 2003.
[12] A. Biswas, V. Vilnrotter, W. Farr, and D. Fort, and E. Sigman, "Pulse position modulated (PPM) ground receiver design for optical communications from deep space," *Proc. SPIE*, vol. 4635, pp. 224–235, 2002.
[13] D. M. Boroson and B. S. Robinson, "The lunar laser communication demonstration: NASA's first step toward very high data rate support of science and exploration missions," *Space Sci. Rev.*, vol. 185, no. 1–4, pp. 115–128, 2014.
[14] M. M. Willis *et al.*, "Performance of a multimode photon-counting optical receiver for the NASA lunar laser communications demonstration," in *Proc.Int. Conf. Space Opt. Syst. Appl.*, 2012, pp. 1–3.
[15] M. E. Grein *et al.*, "Design of a ground-based optical receiver for the lunar laser communications demonstration," *Proc. Int. Conf. Space Opt. Syst. Appl.*, 2011, pp. 72–78.
[16] A. Korneev *et al.*, "Sensitivity and gigahertz counting performance of NbN superconducting single-photon detectors," *Appl. Phys. Lett.*, vol. 84, no. 26, pp. 5338–5440, 2004.
[17] E. A. Dauler *et al.*, "1.25-Gbit/s photon-counting optical communications using a two element superconducting nanowire single photon detector," *Proc. SPIE*, vol. 6372, pp. 1–8, 2006.
[18] Dauler, E. A. *et al.*, "Review of superconducting nanowire single-photon detector system design options and demonstrated performance," *Opt. Eng.* vol. 53, no. 8, 2014, Art. no. 081907.
[19] M. E. Grein, E. A. Dauler, B. S. Robinson, and D. M. Boroson, "An optical receiver for the lunar laser communication demonstration based on photon-counting superconducting nanowires," *Proc. SPIE*, vol. 9492, no. 949208, pp. 1–8, 2015.
[20] F. Bellei *et al.*, "Free-space-coupled superconducting nanowire single-photon detectors for infrared optical communications," *Opt. Exp.*, vol. 24, no. 4, pp. 3248–3257, 2016.
[21] N. R Gemmell *et al.*, "A miniaturized 4K platform for superconducting infrared photon counting detectors," *Superconductor Sci. Technol.*, no. 30, p. 11LT01, 2014.
[22] L. You *et al.*, "Superconducting nanowire single photon detection system for space applications," *Opt. Exp.*, vol. 26, no. 3, pp. 2965–2971, 2018.
[23] S. Dolinar, D. Divsalar, and J. Hamkins, "Capacity of pulse-position modulation (PPM) on Gaussian and Webb channels," *Interplanetary Netw. Prog. Rep.*, vol. 142, no. 89, pp. 314–317, 2000.
[24] X. Yan *et al.*, "Model of bit error rate for laser communication based on superconducting nanowire single photon detector," *Acta Physica Sinica*, vol. 66, no. 19, pp. 320–326, 2017.
[25] A Engel, A. Semenov, H. W. Hübers, K. Ilin, and M. Siegel, "Dark counts of a superconducting single-photon detector," *Nuclear Instrum. Methods Phys. Res.*, vol. 520, no. 1–3, pp. 32–35, 2004.
[26] A. Engel and A. Schilling, "Numerical analysis of detection-mechanism models of SNSPD," *J. Appl. Phys.*, vol. 114, no. 21, pp. 609–R, 2013.
[27] H. Shibata, K. Shimizu, H. Takesue, and Y. Tokura, "Superconducting nanowire single-photon detector with ultralow dark count rate using cold optical filters," *Appl. Phys. Exp.*, vol. 6, no. 7, 2013, Art. no. 072801.
[28] X. Yang *et al.*, "Superconducting nanowire single photon detector with on-chip bandpass filter," *Opt. Exp.*, vol. 22, no. 13, pp. 16268–16272, 2014.
[29] A. Engel, J. J. Renema, K. Il'in, and A. Semenov, "Detection mechanism of superconducting nanowire single-photon detectors," *Superconductor Sci. Technol.*, vol. 28, no. 11, 2015, Art. no. 114003.
[30] A. Engel, A. D. Semenov, H.-W. Hubers, K. Il'in, and M. Siegel, "Fluctuation effects in superconducting nanostrips," *Phys. C Supercond. Appl.*, vol. 444, no. 1–2, pp. 12–18, 2006.
[31] L. You, "Recent progress on superconducting nanowire single photon detector," *Sci. China Inf. Sci.*, vol. 44, no. 3, pp. 370–388, 2014.
[32] N. Bulaevskii, M. J. Graf, and C. D. Batista, "Vortex-induced dissipation in narrow current-biased thin-film superconducting strips," *Physical Rev. B*, vol. 83, no. 14, pp. 4400–4408, 2011.
[33] J. J. Renema *et al.*, "Experimental test of theories of the detection mechanism in a nanowire superconducting single photon detector," *Phys. Rev. Lett.*, vol. 112, no. 11, 2014, Art. no. 117604.
[34] H. Hemmati, *Deep Space Optical Communication*. Hoboken, NJ, USA: Wiley, 2006, ch.4.
[35] M. A. Kashani and M. Kavehrad, "A novel statistical channel model for turbulence-induced fading in free-space optical systems," *J. Lightw. Technol.*, vol. 33, no. 11, pp. 2303–2312, Jun. 2015.
[36] M. Srinivasan *et al.*, "Photon counting detector array algorithms for deep space optical communications," *Proc. SPIE.*, vol. 9739, no. 97390X, pp. 1–16, 2016.